UC Berkeley
UC Berkeley Previously Published Works

Title
Chelation and stabilization of berkelium in oxidation state plus IV

Permalink
https://escholarship.org/uc/item/9zn3q96n

Journal
NATURE CHEMISTRY, 9(9)

ISSN
1755-4330

Authors
Deblonde, Gauthier J-P
Sturzbecher-Hoehne, Manuel
Rupert, Peter B
et al.

Publication Date
2017

DOI
10.1038/NCHEM.2759

Peer reviewed

eScholarship.org Powered by the California Digital Library
University of California

Remarkable complexation and stabilization of berkelium(IV) by a synthetic siderophore: An experimental and theoretical comparison with neighboring trivalent actinide elements

Gauthier J-P. Deblonde[1], Manuel Sturzbecher-Hoehne[1], Peter B. Rupert,[2] Dahlia D. An,[1] Marie-Claire Illy,[1] Corie Y. Ralston,[3] Jiri Brabec,[4] Wibe A. de Jong[*],[5] Roland K. Strong[*],[2] and Rebecca J. Abergel[*1]

[1] *Chemical Sciences Division, Lawrence Berkeley National Laboratory, Berkeley, California 94720, USA*

[2] *Division of Basic Science, Fred Hutchinson Cancer Research Center, Seattle, WA 98109, USA*

[3] *Berkeley Center for Structural Biology, Lawrence Berkeley National Laboratory, Berkeley, CA 94720, USA*

[4] *J. Heyrovsky Institute of Physical Chemistry, 18223 Prague 8, Czech Republic*

[5] *Computational Research Division, Lawrence Berkeley National Laboratory, Berkeley, CA 94720, USA*

Keywords: Berkelium; Californium; Actinides; Chelation; Separation; Luminescence; Sensitization

Abstract

Despite theoretical assertions of berkelium (Bk) being the only transplutonium element that can exhibit +III and +IV oxidation states in solution, evidence of a stable oxidized Bk chelate has so far been elusive. Using a siderophore derivative, stabilization of the heaviest 4+ ion of the periodic table was achieved under mild aqueous conditions. The resulting Bk(IV) complex exhibits unprecedented sensitized luminescence through ligand-to-metal energy transfer, but also inhibits Bk interactions with the protein siderocalin, a mammalian metal transporter. Formation of this neutral Bk(IV) coordination compound contrasts sharply with the corresponding negatively charged species incorporating neighboring trivalent americium, curium and californium (Cf), which are sequestered by siderocalin, as evidenced by Xray diffraction analysis of the Cf(III)-ligand-protein ternary adduct, the first example and crystallographic characterization of a Cf macromolecular assembly. Combined with theoretical predictions, these data open a chapter in transplutonium chemistry and prepare for innovative Bk separation and purification processes.

Introduction

Berkelium (Bk) chemistry is largely unexplored compared to other transplutonium (trans-Pu) elements encountered in measurable amounts in nuclear chemistry, namely americium (Am), curium (Cm), and californium (Cf). Element 97, Bk is a peculiar case in the actinide (An) series because it is "light" enough to be formed by multiple neutron-capture processes during nuclear detonations or in today's nuclear fission reactors, to such extent that it raises concerns for nuclear waste management [1,2]. However, its only isotope available in bulk quantities, ^{249}Bk, has a relatively short half-life of 330 days, which hinders its use in chemical studies. In contrast, ^{243}Am ($t_{1/2}$ = 7,370 yr) and ^{248}Cm ($t_{1/2}$ = 340,000 yr) are long-lived isotopes that can be produced and purified on the multi-gram scale. Likewise, Cf (Z = 98), although heavier than Bk, is easier to synthesize and investigate thanks to the relatively stable isotopes ^{249}Cf ($t_{1/2}$ = 351 yr) and ^{252}Cf ($t_{1/2}$ = 2.65 yr). A consequence of its extreme rarity as a laboratory material and its highly radioactive nature, very few Bk coordination compounds have been characterized to date[3,4] and little is known about the behavior of Bk in environmentally and biologically relevant species.[5,6] Due to the special stability afforded by the half-filled $5f^7$ electronic configuration, Bk is the element among the actinides heavier than Pu that can most readily be oxidized from oxidation state +III to +IV in aqueous systems; its neighboring elements, Am, Cm, Cf, and Es having only limited or inexistent stability as M^{4+} ions.[7] Even though rutherfordium (Rf, Z = 104) is expected to exhibit coordination chemistry properties similar to those of zirconium and hafmium and would therefore also readily form a stable M^{4+} ion in solution,[8] its isotopes are short-lived (from μs to ~1.3 h half-lives) and Bk is, until now, the heaviest element of the periodic table available for bulk chemistry that can be studied as a tetravalent ion. It preferentially exists in aqueous solutions as Bk^{3+} but oxidation to Bk^{4+} under very drastic conditions was reported shortly after the discovery of the element.[9,10] The standard oxidation potential for the couple Bk^{4+}/Bk^{3+} is +1.60 V (in 1 M $HClO_4$, *vs*. NHE),[11] which makes the formation of Bk^{4+} species arduous, yet feasible, with a large excess of very strong oxidizers such as bromate, bismuth trioxide, and lead dioxide, or by prolonged electrolytic oxidation. The redox properties of Bk are relatively close to those of cerium (Ce, $E°Ce^{4+}/Ce^{3+}$ = +1.7 V) and differ significantly from what is observed with the corresponding

lanthanide (Ln) ion, terbium (Tb, $E°Tb^{4+}/Tb^{3+}$ = +3.3 V).[12] This ambivalence, if adequately unlocked, would confer to Bk a chemical behavior readily different from that of adjacent ions, Cm and Cf, whose only stable oxidation state in solution is +III.

Classical attempts to extend the chemistry of Bk have yielded a decrease of the Bk^{4+}/Bk^{3+} potential to +1.56 V in 1 M HNO_3 and +1.37 V in 1 M H_2SO_4.[3,13] An almost identical trend is known for the couple Ce^{4+}/Ce^{3+}, whose redox potential is +1.70 V, +1.61 V, +1.44 V, and +1.28 V in 1 M $HClO_4$, HNO_3, H_2SO_4, and HCl, respectively.[14] The difference in stability between the Bk(IV) and Bk(III) species formed with these common anions is, however, not strong enough to make Bk(IV) readily accessible. In fact, once tremendous efforts are made to oxidize Bk(III) in these mineral acids, Bk(IV) complexes are naturally reduced within a few hours or even minutes.[15–17] More exotic approaches to stabilize Bk(IV) have used saturated pyrophosphate solutions,[17] acidic mixtures of bromate and heteropolytungstate $K_{10}P_2W_{17}O_{61}$,[18] or triphenylarsine oxide in pure acetonitrile,[19] all transient and difficult systems to implement in separation processes or for the sequestration of Bk *in vivo*. A more realistic strategy was proposed in the early 1970's using highly concentrated carbonate solutions,[13,16] with a conditional oxidation potential Bk^{4+}/Bk^{3+} of +0.26 V in 2 M K_2CO_3 (pH 10). Aside from requiring a tremendous excess of carbonate ions, this medium's drawbacks include a narrow pH-range under which Bk(IV) species are stable, the presence of multiple species with unknown stoichiometry or stability,[20] the limited solubility of carbonate salts, and its incompatibility with *in vivo* conditions or most nuclear waste treatment operations in acidic media.

Instead of using large excesses of inorganic complexing ions, we selected a water-soluble small organic molecule that is highly selective toward An(IV) ions in order to lift the thermodynamic barrier imposed by the high redox potential of the couple Bk^{4+}/Bk^{3+}. The synthetic siderophore analog 3,4,3-LI(1,2-HOPO) (Figure 1) has caught growing attention as a therapeutic decorporation agent for its bio-compatibility, its low toxicity,[21–23] and its strong efficiency at sequestering An and Ln ions, including UO_2^{2+}, Ln^{3+}, An^{3+}, Th^{4+}, and Pu^{4+}.[24–27] The hard donor octadentate ligand 3,4,3-LI(1,2-HOPO) binds d- and f-block metal ions through its four 1-hydroxy-pyridine-2-one (1,2-HOPO) functionalities with extremely high affinities (Supplementary Table S1). Besides its ability to chelate

both M(III) and M(IV) ions, a great advantage of 3,4,3-LI(1,2-HOPO) is the unprecedented stability difference between its M(III) and M(IV) complexes, as epitomized by the Ce(III) complex that exhibits a formation constant of $10^{+17.4}$, 24 orders of magnitude lower than that of its Ce(IV) counterpart ($10^{+41.5}$).[28] This strong stabilization of Ce(IV), with a free energy of formation of -240 kJ.mol^{-1} compared to -99.3 kJ.mol^{-1} for the Ce(III) complex, compensates the energetic barrier imposed by the redox potential of Ce^{4+}/Ce^{3+} (124 kJ.mol^{-1}) for the free ion. Thus the redox potential of the [Ce^{IV}3,4,3-LI(1,2-HOPO)]/[Ce^{III}3,4,3-LI(1,2-HOPO)]$^{-}$ system decreases to -0.02 V,[28] from the free ion's +1.28 V. So far, no other man-made ligand combines such high stability for both M(III) and M(IV) complexes with extreme selectivity toward M(IV) ions.

Results and Discussion

Bk redox potentials being usually 50 to 100 mV lower than their Ce counterparts,[3] the redox potential for $[Bk^{IV}$3,4,3-LI(1,2-HOPO)]/$[Bk^{III}$3,4,3-LI(1,2-HOPO)]$^-$ is expected to be around -0.1 V (*vs*. NHE), suggesting an easy and direct access to Bk(IV) in solution. This estimated value was confirmed by density functional theory (DFT) calculations on both gas-phase and solvated Bk(III) and Bk(IV) species, for which coordinates and frequencies of the calculated species are listed in Supplementary Tables S2-S7; in those solvated species, a Bk^{4+}/Bk^{3+} electrochemical potential with an upper bound of -0.13 V relative to NHE was determined. Considering trends in An ionic radii[29] and corresponding Th(IV) and Pu(IV) complex stability constants, a formation constant of $10^{+44.7}$ (at 25°C) is estimated for $[Bk^{IV}$3,4,3-LI(1,2-HOPO)], a drastic increase over $[Bk^{III}DTPA]^{2-}$ (DTPA = diethylenetriaminepentaacetic acid, log $\beta_{110} = 10^{+22.8}$) and $[Bk^{III}DPA_3]^{3-}$ (DPA = dipicolinic acid, log $\beta_{130} = 10^{+23.1}$), currently the most stable known Bk coordination compounds.[4,30] Rigorous metal or ligand-competition assays commonly used to determine thermodynamic constants for other 4^+ metal complexes cannot be applied to Bk(IV) as they would necessitate a competing ligand that could stabilize Bk(IV) once released by 3,4,3-LI(1,2-HOPO), with a known affinity for Bk(IV). Such a system is currently unavailable since 3,4,3-LI(1,2-HOPO) is the first organic ligand reported to stabilize Bk(IV) and no thermodynamic stability constant for a Bk(IV) aqueous species has ever been established.

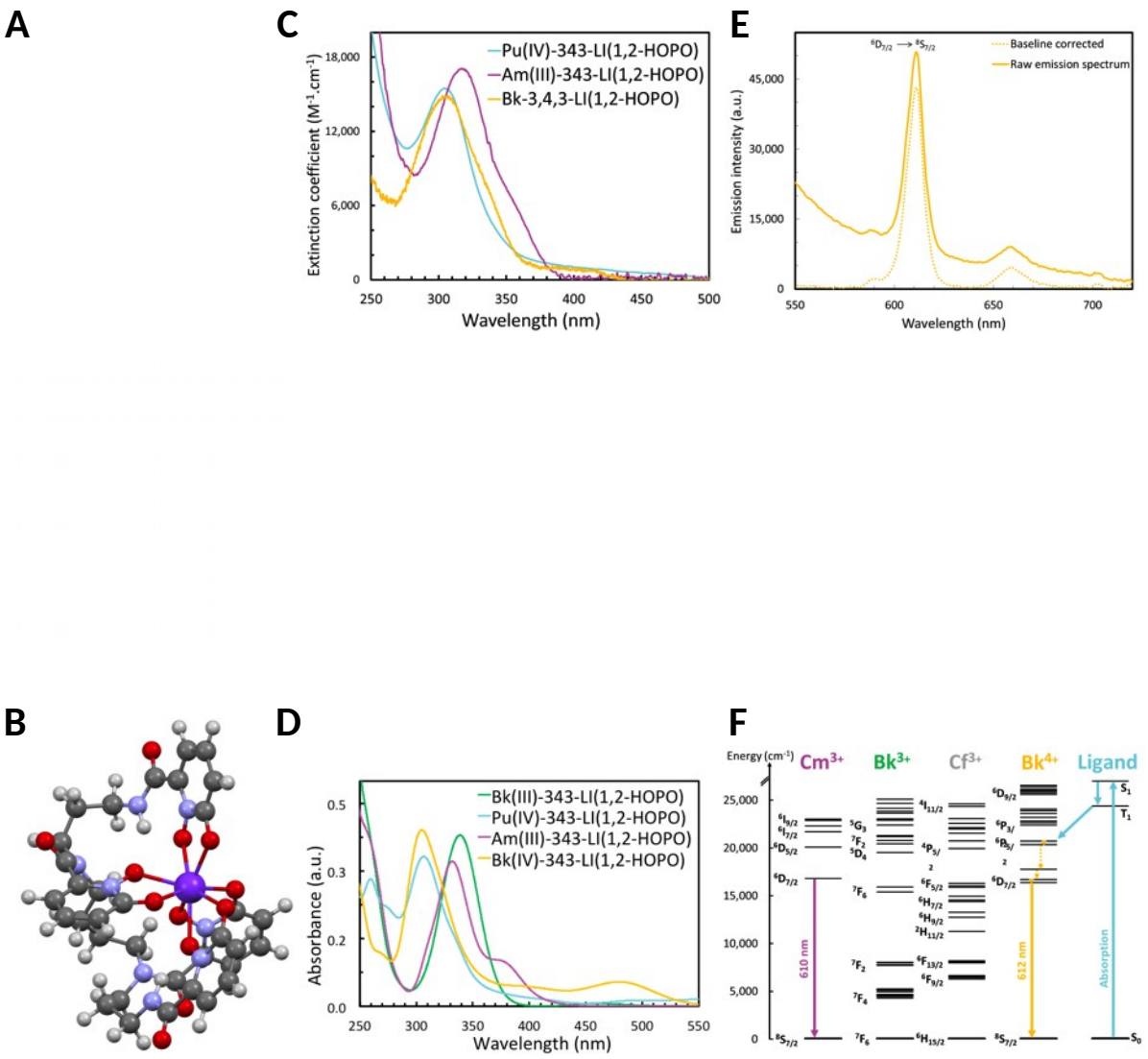

Figure 1. (**A**) Molecular structure of 3,4,3-LI(1,2-HOPO); the hydrogen atoms highlighted in red are labile. (**B**) Computed DFT structure of [Bk^{IV}3,4,3-LI(1,2-HOPO)]. (**C**) Experimental absorbance spectra of 3,4,3-LI(1,2-HOPO) complexes with Pu^{4+} (blue), Am^{3+} (magenta) and Bk (yellow) in aqueous solution. (**D**) Computed absorbance spectra for the Pu^{4+} (Supplementary Table S8), Bk^{4+}, Bk^{3+} (green) and Am^{3+} (Supplementary Table S9) complexes. (**E**) Steady-state emission spectrum of [$^{249}Bk^{IV}$3,4,3-LI(1,2-HOPO)] upon excitation at 320 nm in 0.1 M CHES buffer, pH 8.4, 25°C. (**F**) Jablonski diagrams for the ligand 3,4,3-LI(1,2-HOPO) and Cm^{3+}, Bk^{3+}, Bk^{4+} and Cf^{3+}. Respective Bk^{4+} and An^{3+} energy levels correspond to those reported for Bk(IV)-doped $CeF_{4(s)}$[31] and for $AnCl_3$ or An(III)-doped $LaCl_{3(s)}$.[32]

Stabilization of Bk(IV) by 3,4,3-LI(1,2-HOPO) was first indicated by UV-visible spectrophotometry. A striking difference is observed between the An(III) and An(IV) complexes, with respective absorbance bands centered at 318 and 305 nm, as shown for Am(III) and Pu(IV) (Figure 1C), and the Bk species displaying a maximum absorbance at 305 nm for this sharp band characteristic of the 1,2-HOPO $\pi \rightarrow \pi^*$ transitions. In addition, the Bk complex exhibits a ligand-to-metal charge transfer band centered at 400 nm, a feature also observed with Pu(IV) and Ce(IV) complexes.[26,28] Absorbance spectrum assignment to Bk(IV) was further corroborated by theoretical calculations (Figure 1D). Luminescence properties have long proven instrumental for An complex characterization but most studies focused on Cm species, owing to the $5f^7$ electronic configuration and intrinsically intense $^6D_{7/2} \rightarrow {}^8S_{7/2}$ emission of Cm^{3+}, which facilitates direct excitation of f-f transitions. Luminescence studies of Bk species are scarce and limited to the solid-state,[31,33] to the exception of a report on Bk(III) luminescence in 0.5 M DCl [34]. Characterization of [Bk^{IV}3,4,3-LI(1,2-HOPO)] provided the first Bk(IV) luminescence spectral features in aqueous solution via intramolecular sensitization through the so-called antenna effect: ligand excitation at 320 nm resulted in sharp emission peaks at 590, 612, 659 and 702 nm, with the most intense centered at 612 nm (Figure 1E). The corresponding excitation spectrum monitoring emission at 612 nm displayed a main transition centered at 305 nm (Supplementary Figure S1) and characteristic of energy transfer from the ligand 1,2-HOPO units. [27] The observed structured four-peak emission is due to ligand field splitting of the emitting state, J = 7/2, as the spherical symmetry of the half-filled $5f^7$ configuration should only result in a small splitting (945 cm^{-1} between the lowest and highest Stark levels for the free ion *vs* 2,700 cm^{-1} for the chelated ion). Interestingly, the bathochromic shift of the emission maxima typically observed during complexation of Ln and An ions appears very pronounced here: from the highest to the lowest Stark levels of the excited state $^6D_{7/2}$, shifts of ~10 to 90 nm (equivalent to energy shifts of up to 2,100 cm^{-1} or roughly 12%) were observed in the complexation of Bk by 3,4,3-LI(1,2-HOPO). While large shifts (on the order of ~50 nm, or ∼1100 cm−1) have been noted in 5f systems before,[35] the relative decrease in inter-electronic repulsion in this Bk species is remarkable, especially when compared with the corresponding Am(III)[27] and Cm(III)[25] species that displayed respective relative shifts of the order of 1% and 2.5%.

These features bestow additional evidence of the stabilization of Bk(IV) by 3,4,3-LI(1,2-HOPO) since, based-on the reported energy levels of Bk(III), the ligand cannot sensitize Bk(III) (Figure 1F). Correspondingly, excitation of the ligand in $[Cf^{III}$3,4,3-LI(1,2-HOPO)$]^-$ did not result in any luminescence features, as expected from the energy levels of Cf(III). The main emission of $[Bk^{IV}$3,4,3-LI(1,2-HOPO)] (612 nm, $\Phi = 1.2 \times 10^{-5}$) is consistent with the 611 fluorescence band reported for solid Bk-doped CeF_4 after direct excitation[31] and is close to, but completely distinct from, that reported for the isoelectronic Cm(III) complex (610 nm, $\Phi = 0.45$[25]). Despite the similar half-filled $5f^7$ configurations of both metal ions, the stronger spin-orbit coupling associated with Bk^{4+} (ζ = 3244 for the free ion[36]) gives rise to metal-centered electronic energy levels closer to each other than in the case of Cm^{3+} (ζ = 2889[32]). Hence the much lower ligand-to-metal energy transfer efficiency observed for the Bk(IV) species is most likely due to the induced presence of a large number of non-emissive energy levels between the ligand triplet excited state and the metal $^6D_{7/2}$ emitting state (Figure 1F). The Bk(IV) complex displayed a bi-exponential luminescence decay (Supplementary Figure S2) with two distinct lifetimes (188 ± 19 µs and 6.7 ± 0.9 µs), both increasing slowly but linearly with D_2O content in solution (Supplementary Table S10) and shorter than but in the same range as that of the Cm(III) complex (383 ± 38 µs), consistent with a hardly smaller gap between the $^6D_{7/2}$ emitting and $^8S_{7/2}$ accepting levels for Bk.

The Bk oxidation state when bound to 3,4,3-L(1,2-HOPO) was unambiguously assigned through liquid chromatography (LC) coupled with high resolution mass spectrometry (MS). Analysis of 1:1 metal:ligand aqueous mixtures prepared under ambient conditions with ^{241}Am(III), ^{248}Cm(III) and ^{249}Cf(III), whose M^{4+}/M^{3+} redox potentials are extremely high (+2.6, +3.1 and +3.2 V, respectively)[7,37] confirmed the formation of trivalent 3,4,3-LI(1,2-HOPO) complexes. For those three trans-Pu elements, MS patterns are almost identical, with four mono-charged adducts detected ($[M^{III}LH_2]^+$, $[M^{III}LHNa]^+$, $[M^{III}LNa_2]^+$ and $[M^{III}LNaK]^+$), which clearly contrasts with the data obtained for tetravalent ^{242}Pu and ^{232}Th complexes (Figures 2 and S3). The MS spectrum of the ^{249}Bk system assembled *in situ* from a $Bk^{III}Cl_3$ solution displayed $[BkLH]^+$, $[BkLNa]^+$ and $[BkLK]^+$ species, demonstrating that the resulting complex contains a Bk(IV) ion and not Bk(III) (Figure 2).

Spontaneous stabilization of Bk(IV) is thought to occur through air oxidation, similarly to the Ce system, which does not necessitate the addition of oxidizers or the electrolytic oxidation required in previously proposed methods. The use of 3,4,3-LI(1,2-HOPO) as a chelation and oxidation-promoting agent for Bk(III) also has the notable advantage of promoting the formation of M(IV) species over a wide pH-range: the Zr(IV), Ce(IV) and Pu(IV) complexes are formed in 1 M H_2SO_4[26] and are stable up to pH 11 (Supplementary Figure S4). Finally, the very high formation constants of the M^{IV}3,4,3-LI(1,2-HOPO) complexes prevent competition with any ligand potentially present in the media which gives more flexibility and robustness to the system.

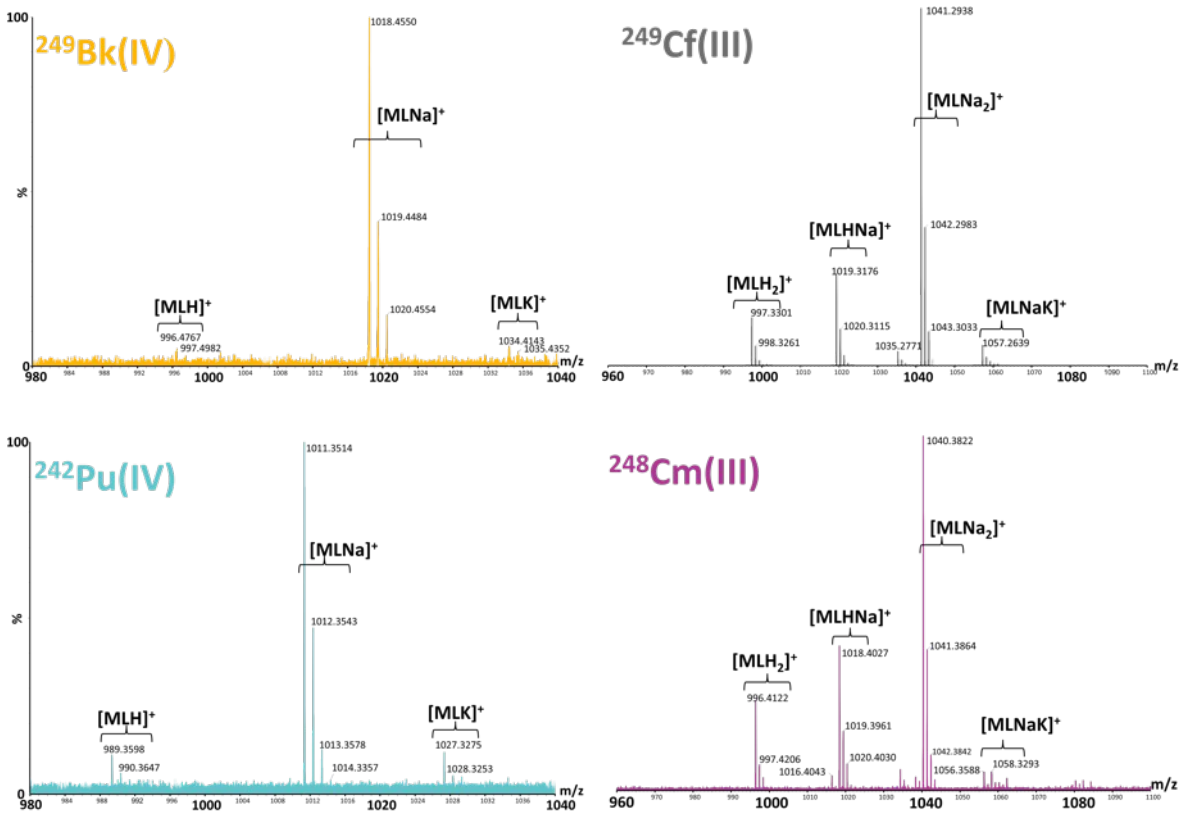

Figure 2. High resolution mass spectra of 3,4,3-LI(1,2-HOPO)$^{4-}$ (L) solutions containing 1 equivalent of ^{242}Pu, ^{248}Cm, ^{249}Cf or ^{249}Bk; detection in positive mode.

Stabilization of Bk(IV) by 3,4,3-LI(1,2-HOPO) was further confirmed using secondary macromolecular recognition. The human protein siderocalin (Scn), known to intercept ferric complexes of microbial siderophores as an immune response against bacterial invasion and recently highlighted as a potential player in actinide mammalian uptake, specifically recognizes negatively charged Ln(III), Am(III) and Cm(III) complexes of 3,4,3-LI(1,2-HOPO)[38] through tight electrostatic interactions, but not the neutral Th(IV) and Pu(IV) analogs. A fluorescence quenching assay revealed Scn does not recognize Bk-3,4,3-LI(1,2-HOPO), evidencing the complex neutrality and indirectly confirming the stabilization of Bk(IV) and not Bk(III) by 3,4,3-LI(1,2-HOPO). In contrast, [Cf^{III}3,4,3-LI(1,2-HOPO)]$^-$ bound Scn with an equilibrium dissociation constant K_d of 50 ± 5 nM, which is in the same range as those reported for Am(III) and Cm(III) (29 and 22 nM, respectively).[38] The structure of the [$^{249}Cf^{III}$3,4,3-LI(1,2-HOPO)]/Scn ternary complex was determined (Supplementary Table S11) using methods analogous to those derived for corresponding Ln (Sm) and An (^{243}Am, ^{248}Cm) metal/chelator/Scn adducts;[38] it is the first crystallographic report of a macromolecular Cf assembly. Those prior structures demonstrated that octadentate complexes bind the trilobal Scn ligand binding site, or “calyx”, much as native ferric siderophore complexes do, with 1,2-HOPO units fitting snuggly into sub-pockets within the calyx (Figure 3A). The overall ^{249}Cf(III) structure is very similar, particularly with regard to the protein (Figure 3B). However, in detail, the 1,2-HOPO subunits of the chelator showed much more variability among the three views of the [$^{249}Cf^{III}$3,4,3-LI(1,2-HOPO)]$^-$ complex (z = 3) than among the 18 near-identical views (six per crystallographic asymmetric unit, z = 6) of the previous three complex structures (Sm, ^{243}Am, ^{248}Cm, Figure 3C). The octadentate coordination around the Sm, ^{243}Am, and ^{248}Cm centers that was best described as a “snub disphenoid” was altered in the case of ^{249}Cf, resulting in incomplete coordination of the ^{249}Cf(III) center by two of the 1,2-HOPO groups; likely due to different bond lengths between metals and 1,2-HOPO groups constrained to bind within the rigid calyx (Supplementary Table S11). The coordination differences between the Sm and ^{249}Cf structures are noteworthy, as both metal ions are comparably sized,[39] and suggest that the Cf 5f orbitals may participate in increased orbital mixing.

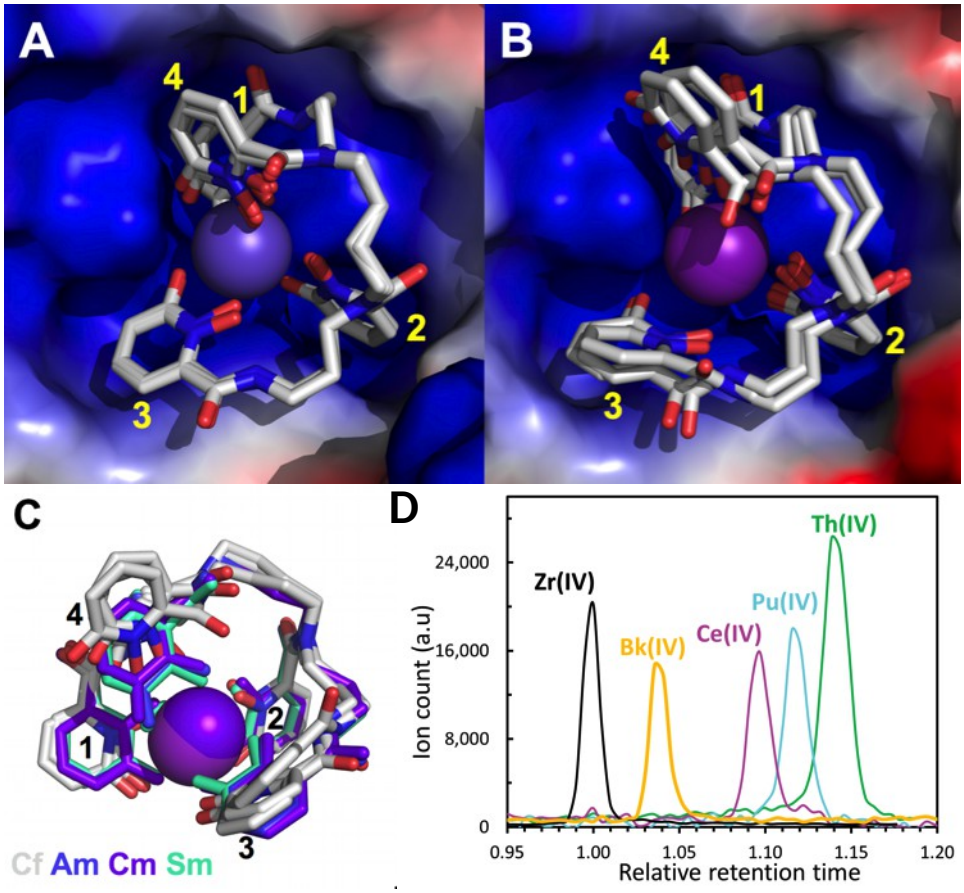

Figure 3. (**A**) Views of previous Scn/[M^{III}3,4,3-LI(1,2-HOPO)]$^{-}$ complex structures show a high degree of structural conservation, with the metal centers ($^{243}Am^{3+}$, $^{248}Cm^{3+}$, Sm^{3+}) rendered as CPK spheres, the chelator represented by licorice-stick, and the molecular surface of Scn colored by electrostatic potential (blue: positive, red: negative). Only one of six independent views from each of the three separate structures is shown in this superposition. HOPO groups are numbered, with group #1 sitting in the key pocket defining the Scn recognition mechanism,[38] partially obscured in this orientation. (**B**) Views of the superposition of the three complexes in the asymmetric unit of the Scn/[$^{249}Cf^{III}$3,4,3-LI(1,2-HOPO)]$^{-}$ structure, rendered as in (A), show a greater degree of structural variation among the three ^{249}Cf complexes in the crystal than across the three previous complex structures. The #4 HOPO group is clearly displaced outwards from the calyx. (**C**) A superposition, based on the structures of Scn, shows the structural differences between one each of the $^{243}Am^{3+}$, $^{248}Cm^{3+}$, and Sm^{3+} 3,4,3-LI(1,2-HOPO) complexes (colored as indicated) and the three ^{249}Cf/3,4,3-LI(1,2-HOPO) complexes (colored by atom type). Incomplete coordination of the ^{249}Cf atom by the #3 and #4 HOPO groups is apparent. (**D**) Relative chromatographic retention of [Ce^{IV}3,4,3-LI(1,2-HOPO)], [$^{232}Th^{IV}$3,4,3-LI(1,2-HOPO)], [$^{242}Pu^{IV}$3,4,3-LI(1,2-HOPO)], and [$^{249}Bk^{IV}$3,4,3-LI(1,2-HOPO)], relative to [Zr^{IV}3,4,3-LI(1,2-HOPO)], on an XDB-C18 column. Detection achieved by mass spectrometry (m/z = 859, 909, 1001, 1011, 1018 for Zr, Ce, Th, Pu, Bk, respectively).

Current processes to separate Bk from Am, Cm, Cf, and fission products after production necessitate numerous steps and use strong oxidizers such as bromate to segregate Bk(IV) from the non-tetravalent ions.[3] Liquid-liquid extraction steps involving mixed mineral acid and organic solvents as well as multiple final separation steps using ion-exchange columns are almost always included in those processes [3,40], even in the case of more recently reported rapid separation techniques [41]. The non-recognition of [Bk^{IV}3,4,3-LI(1,2-HOPO)] by Scn suggests innovative procedures to separate Bk from M(III) ions could consist of passing a 3,4,3-LI(1,2-HOPO) solution of the irradiated mixture through a Scn-containing medium, followed by discrimination using either size, mass, affinity, polarity or solubility differences. However, the separation of Bk(IV) from other M(IV) ions potentially present during Bk production, namely Zr, Ce, Th and Pu, also presents a challenge. The Ce-Bk pair is currently known as the most difficult due to the almost-identical redox properties of the two elements,[3] which has led to complicated solvent extraction or ion exchange techniques.[42–46] Figure 3D displays the relative retention of various M(IV) complexes of 3,4,3-LI(1,2-HOPO) on a classical C18 LC column. The retention time of the Bk complex falls between those of Zr(IV) and Ce(IV), trending with the ionic radii of the octa-coordinated metals (0.84, 0.93, and 0.97 pm for Zr^{4+}, Bk^{4+} and Ce^{4+}, respectively).[29] Without actual optimization, [Bk^{IV}3,4,3-LI(1,2-HOPO)] was easily discriminated from its Ce, Th and Pu analogs. Hence, a two-step separation process is sufficient for isolating Bk from all other Ln and An ions, with step 1 sequestering 3^+ ions based on Scn selectivity toward [M^{III}3,4,3-LI(1,2-HOPO)]$^-$ complexes, and step 2 separating Bk from 4^+ ions under classical chromatography. Besides stabilizing the heaviest +IV ion of the periodic table available for bulk chemistry, this procedure represents tremendous progress for Bk chemistry as it keeps Bk species in aqueous phase throughout the process, is operated at room temperature, and does not introduce additional non-volatile elements or require any biphasic liquid-liquid extraction step, with limiting variables such as solvent loading capacity, pH robustness, extractant solubility, third-phase formation, etc. Recovery of Bk from the final eluted solutions would be achieved either through acidification and ashing or by precipitation of Bk-hydroxide species upon pH increase and subsequent filtration. Both methods (ashing or precipitation), commonly used in hydrometallurgy and would allow recovery of solid Bk.

Finally, the protein/ligand-based separation strategy described here could be used to design cleaner and softer methods for metal ion sorting based on bioengineered systems.

Materials and methods

Caution: ^{249}Cf (half-life of 351 years; specific activity: 4.1 Ci.g^{-1}) represents a serious health risk owing to its α emission (6.194 MeV) and, more importantly, its γ emission (0.388 MeV), as well as the emission of its decay products. ^{249}Cf decays to ^{245}Cm (half-life of 8,500 years), which is an α emitter (5.623 MeV) and undergoes spontaneous fission *i.e.* emitting a large flux of neutrons. ^{249}Bk (half-life of 330 days) is a β emitter that decays to ^{249}Cf therefore representing a serious health risk too. ^{248}Cm (half-life of 3.49x10^5 years; 5.162 MeV) and ^{242}Pu (half-life of 3.74x10^5 years; 4.985 MeV) are α emitters and represent serious health risks. All these radioactive elements where manipulated in laboratories specially designed for the safe handling of transuranium elements.

Materials. Chemicals were acquired from commercial suppliers and were used as received. The ligands 3,4,3-LI(1,2-HOPO) was prepared and characterized as previously described.[47] Stock solutions (4 mM) of 3,4,3-LI(1,2-HOPO) were prepared by direct dissolution of a weighed portion of ligand in DMSO and aliquots were removed prior to each set of experiments. Aliquots of acidified stocks of carrier-free ^{249}Cf and ^{248}Cm (95.78% ^{248}Cm, 4.12% ^{246}Cm, 0.06% ^{245}Cm, 0.02% ^{244}Cm/^{247}Cm isotopic distribution by atom percentage) from the Lawrence Berkeley National Laboratory were used in this work. A stock solution of ^{249}Bk(III) in 0.1 M HCl was prepared from solid $^{249}BkCl_3$ obtained from the Oak Ridge National Laboratory. All measurements reported here were completed within six weeks of the original separation work and within two weeks of dissolution of the dry salt. All aqueous solutions were prepared using deionized water purified by a Millipore Milli-Q reverse osmosis cartridge system and the pH was adjusted as needed with concentrated HCl or KOH. The pH of solutions was measured with a conventional pH meter at 25°C (Metrohm Brinkmann) that was equipped with a glass electrode (Micro Combi, Metrohm) filled with KCl and calibrated with pH standards. For direct spectroscopic measurements, equimolar amounts of metal and chelator were used to constitute complex solutions (40 μM, pH 8.4) in 0.1 M CHES buffer. Recombinant human Scn was prepared as previously described.[48]

Liquid Chromatography - Mass Spectrometry. Liquid chromatography-high resolution mass spectrometry (LC-HRMS) spectra were acquired on a UPLC Waters Xevo system interfaced with a

QTOF mass spectrometer (Waters Corporation, Milford, MA, USA) in Micromass Z-spray geometry. The experimental setting used for LC-HRMS assays has been previously described (see Supplementary Information)[26] and was applied to samples containing an equal concentration of actinide and 3,4,3-LI(1,2-HOPO) prepared in 0.1 M HEPES buffer at pH 7.4 (for Cm, Cf and Bk) or in 0.5% formic acid at pH 2 (for Ce, Th, and Pu). The concentrations used were 10 μM for ^{243}Am, ^{249}Bk and ^{249}Cf samples and 1 μM for Ce, ^{232}Th, ^{242}Pu, and ^{248}Cm.

Protein Fluorescence Quenching Binding Assay. The affinity of siderocalin for 3,4,3-LI(1,2-HOPO) complexes was quantified by monitoring the intrinsic fluorescence of the protein upon complex-binding as described previously[38] and detailed in Supplementary Information.

Photophysics. UV-visible absorption spectra were recorded either on an Ocean Optics USB 4000 absorption spectrometer, using quartz cells of 1.00 cm path length. Emission spectra were acquired on a HORIBA Jobin Yvon IBH FluoroLog-3 spectrofluorimeter, used in steady state mode. Luminescence lifetimes were determined on a HORIBA Jobin Yvon IBH FluoroLog-3 spectrofluorimeter, adapted for time-correlated single photon counting (TCSPC) and multichannel scaling (MCS) measurements. Further experiment and instrument details are provided in Supplementary Information.

Crystallography. For crystallization, 1 mM solutions of equimolar Cf-3,4,3-LI(1,2-HOPO) complex were mixed in a 2:1 molar ratio with Scn, which was then buffer-exchanged into 25 mM PIPES (pH = 7.0), 150 mM NaCl, 1 mM EDTA, and 0.01% w/w NaN_3, and concentrated to ~10 mg/ml protein. Diffraction-quality crystals were grown by vapor diffusion as detailed in Supplementary Information, along with data collection and refinement methods. Crystallographic statistics are reported in Supplementary Table S11. Final models have been deposited in the PDB.[49]

Computational Chemistry Simulations. All calculations were performed with the latest development version of the open-source NWChem software suite.[50] Scalar relativistic density functional theory calculations were carried out with the B3LYP[51,52] density functional, using the Stuttgart small-core effective core-potential and associated basis set for the actinide atoms[53] and all-electron DFT optimized valence double-ζ polarized (DZVP) basis sets[54] for the light atoms in the

complex. UV-visible spectra were calculated at the time-dependent density functional theory (TDDFT) level of theory.[55] TDDFT equations were solved using a novel new symmetric Lanczos algorithm.[56] Geometries of solutions species were optimized within the COSMO model. The DIRAC code[57] and Dyall's relativistic triple-zeta basis set[58] were used to estimate the effect of atomic spin-orbit coupling on Bk^{4+} with a $5f^7\ ^8S_{7/2}$ ground state, and Bk^{3+} with a $5f^8\ ^7F_6$ ground state at the Dirac-Hartree-Fock level of theory. For each atom an average-of-configurations SCF was performed followed by a Complete Active Space CI (COSCI) in the space covered by the $5f^7$ or $5f^8$ to project out all the states. Additional computational details are provided as Supplementary Information.

References and Notes

1. Kosyakov, V. N. Perspective methods for Berkelium–249 preparation and application. *J. Nucl. Sci. Technol.* **39,** 42–44 (2002).
2. Vértes, A., Nagy, S., Klencsár, Z. & Lovas, R. G. in *Handbook of nuclear chemistry: Instrumentation, separation techniques environmental issues* (Kluwer Academic Publishers, 2003).
3. Hobart, D. E. & Peterson, J. R. *The Chemistry of the Actinide and Transactinide Elements - Chapter X - Berkelium*. (Springer, 2006).
4. Silver, M. A. *et al.* Characterization of berkelium(III) dipicolinate and borate compounds in solution and the solid state. *Science* **353,** (2016).
5. Hungate, F. P. *et al.* Preliminary Data on 252Es and 249Bk Metabolism in Rats. *Health Phys* **22,** 653–656 (1972).
6. Taylor, G. N. *et al.* Microscopic Distribution of Californium-249 and Berkelium-249 in the Soft Tissues of Beagles. *Health Phys* **22,** 691–693 (1972).
7. Runde, W. H. & Mincher, B. J. Higher Oxidation States of Americium: Preparation, Characterization and Use for Separations. *Chem. Rev.* **111,** 5723–5741 (2011).
8. Czerwinski, K. R. Studies of fundamental properties of rutherfordium (element 104) using organic complexing agents. *Lawrence Berkeley Natl. Lab.* (2010).
9. Thompson, S. G., Ghiorso, A. & Seaborg, G. T. Element 97. *Phys. Rev.* **77,** 838 (1950).
10. Thompson, S. G., Cunningham, B. B. & Seaborg, G. T. Chemical properties of Berkelium. *J. Am. Chem. Soc.* **72,** 2798–2801 (1950).
11. Antonio, M. R., Williams, C. W. & Soderholm, L. Berkelium redox speciation. *Radiochim. Acta* **90,** 851–856 (2002).
12. Cotton, S. *Lanthanide and Actinide Chemistry*. (Wiley, 2006).

13. Stokely, J. R., Baybarz, R. D. & Peterson, J. R. The formal potential of the Bk(IV)-Bk(III) couple in several media. *J. Inorg. Nucl. Chem.* **34,** 392–393 (1972).
14. Wadsworth, E., Duke, F. R. & Goetz, C. A. Present status of Cerium (IV)-Cerium (III) potentials. *Anal. Chem.* **29,** 1824–1825 (1957).
15. Gutmacher, R. G. *et al*. The absorption spectra of Bk3+ and Bk4+ in solution. *J. Inorg. Nucl. Chem.* **29,** 2341–2345 (1967).
16. Baybarz, R. D. & Stokely, J. R. Absorption spectra of Bk(III) and Bk(IV) in several media. *J. Inorg. Nucl. Chem.* **34,** 739–746 (1972).
17. Gutmacher, R. G., Bodé, D. D., Lougheed, R. W. & Hulet, E. K. The stability of tetravalent berkelium in acid solution and the absorption spectra of Bk(IV) and Bk(III). *J. Inorg. Nucl. Chem.* **35,** 979–994 (1973).
18. Milyukova, M. S., Malikov, D. A., Kuzovkina, E. V. & Myasoedov, B. F. Extraction of Bk(IV) with POM - Milyukova, 1986.pdf. *J. Radioanal. Nucl. Chem.* **104,** 81–90 (1986).
19. Payne, G. F. & Peterson, J. R. Possible stabilization of the tetravalent oxidation state of berkelium and californium in acetonitrile with triphenylarsine oxide. *Inorganica Chim. Acta* **139,** 111–112 (1987).
20. Morris, D. E., Hobart, D. E. & Palmer, P. D. Voltammetric investigation of the berkelium(IV/III) couple in concentrated aqueous carbonate solutions. *Radiochim. Acta* **49,** 125–134 (1990).
21. Bunin, D. I. *et al*. Dose-Dependent Efficacy and Safety Toxicology of Hydroxypyridinonate Actinide Decorporation Agents in Rodents: Towards a Safe and Effective Human Dosing Regimen. *Radiat. Res.* **179,** 171–182 (2013).

22. Choi, T. A. *et al*. Biodistribution of the Multidentate Hydroxypyridinonate Ligand [^{14} C]-3,4,3-LI(1,2-HOPO), a Potent Actinide Decorporation Agent: BIODISTRIBUTION OF 3,4,3-LI(1,2-HOPO). *Drug Dev. Res.* **76,** 107–122 (2015).
23. Choi, T. A. *et al*. In Vitro Metabolism and Stability of the Actinide Chelating Agent 3,4,3-LI(1,2-HOPO). *J. Pharm. Sci.* **104,** 1832–1838 (2015).
24. Sturzbecher-Hoehne, M., Deblonde, G. J.-P. & Abergel, R. J. Solution thermodynamic evaluation of hydroxypyridinonate chelators 3,4,3-LI(1,2-HOPO) and 5-LIO(Me-3,2-HOPO) for UO2(VI) and Th(IV) decorporation. *Radiochim. Acta* **101,** 359–366 (2013).
25. Sturzbecher-Hoehne, M., Kullgren, B., Jarvis, E. E., An, D. D. & Abergel, R. J. Highly Luminescent and Stable Hydroxypyridinonate Complexes: A Step Towards New Curium Decontamination Strategies. *Chem. - Eur. J.* **20,** 9962–9968 (2014).
26. Sturzbecher-Hoehne, M., Choi, T. A. & Abergel, R. J. Hydroxypyridinonate Complex Stability of Group (IV) Metals and Tetravalent f-Block Elements: The Key to the Next Generation of Chelating Agents for Radiopharmaceuticals. *Inorg. Chem.* **54,** 3462–3468 (2015).
27. Sturzbecher-Hoehne, M., Yang, P., D'Aléo, A. & Abergel, R. J. Intramolecular sensitization of americium luminescence in solution: shining light on short-lived forbidden 5f transitions. *Dalton Trans* (2016). doi:10.1039/C6DT00328A
28. Deblonde, G. J.-P., Sturzbecher-Hoehne, M. & Abergel, R. J. Solution Thermodynamic Stability of Complexes Formed with the Octadentate Hydroxypyridinonate Ligand 3,4,3-LI(1,2-HOPO): A Critical Feature for Efficient Chelation of Lanthanide(IV) and Actinide(IV) Ions. *Inorg. Chem.* **52,** 8805–8811 (2013).
29. Shannon, R. . Revised effective ionic radii and systematic studies of interatomic distances in halides and chalcogenides. *Acta Crystallogr. A* **32,** 751–767 (1976).

30. Baybarz, R. D. Dissociation constants of the transplutonium element chelates of diethylnetriaminepentaacetic acid (DTPA) and the application of DTPA chelates to solvent extraction separations of transplutonium elements from the lanthanide elements. *J. Inorg. Nucl. Chem.* **27,** 1831–1839 (1965).
31. Jursich, G. M. *et al.* Laser induced fluorescence of 249 Bk 4+ in CeF 4. *Inorganica Chim. Acta* **139,** 273–274 (1987).
32. Carnall, W. T. *A systematic analysis of the spectra the trivalent actinide chlorides in D3h site symetry*. (Argonne National Laboratory, 1989).
33. Nugent, L. J. *et al.* Intramolecular energy transfer and sensitized luminescence in actinide (III). beta.-diketone chelates. *J. Phys. Chem.* **73,** 1540–1549 (1969).
34. Carnall, W., Beitz, J. & Crosswhite, H. Electronic energy level and intensity correlations in the spectra of the trivalent actinide aquo ions. III. Bk3+. *J. Chem. Phys.* **80,** 2301–2308 (1984).
35. Barbanel, A. Nephelauxetic effect and hypersensitivity in the optical spectra of actinides. *Radiochim. Acta* **78,** 91–96 (1997).
36. Liu, G., Carnall, W., Jursich, G. & Williams, C. Analysis of the crystal-field spectra of the actinide tetrafluorides. II. AmF4, CmF4, Cm4+: CeF4, and Bk4+: CeF4. *J. Chem. Phys.* **101,** 8277–8289 (1994).
37. Nugent, L. J., Baybarz, R. D., Burnett, J. L. & Ryan, J. L. Electron-transfer and fd absorption bands of some lanthanide and actinide complexes and the standard (II-III) oxidation potential for each member of the lanthanide and actinide series. *J. Phys. Chem.* **77,** 1528–1539 (1973).
38. Allred, B. E. *et al.* Siderocalin-mediated recognition, sensitization, and cellular uptake of actinides. *Proc. Natl. Acad. Sci.* **112,** 10342–10347 (2015).

39. Lundberg, D. & Persson, I. The size of actinoid (III) ions–structural analysis vs. common misinterpretations. *Coord. Chem. Rev.* **318,** 131–134 (2016).
40. Myasoedov, B. & Lebedev, I. Latest achievements in the analytical chemistry of actinides. *J. Radioanal. Nucl. Chem.* **147,** 5–26 (1991).
41. Maruyama, T. *et al*. Rapid Chemical Separation for Bk. *J. Nucl. Radiochem. Sci.* **3,** 155–158 (2002).
42. Peppard, D. F., Moline, S. W. & Mason, G. W. Isolation of berkelium by solvent extraction of the tetravalent species. *J. Inorg. Nucl. Chem.* **4,** 344–348 (1957).
43. Moore, F. L. New method for rapid separation of berkelium (IV) from cerium (IV) by anion exchange. *Anal. Chem.* **39,** 1874–1876 (1967).
44. Moore, F. L. Liquid-liquid extraction method for the separation of cerium (IV) from berkelium (IV) and other elements. *Anal. Chem.* **41,** 1658–1661 (1969).
45. Chudinov, E. G. & Pirozhkov, S. V. The separation of berkelium (III) from cerium (III). *J. Radioanal. Chem.* **10,** 41–46 (1972).
46. Liu, Y.-F. *et al*. Procedures for a fast separation of berkelium from complex mixtures of reaction products. *J. Radioanal. Nucl. Chem.* **76,** 119–124 (1983).
47. Y. Chang, P. *et al*. Analytical Methods for the Bioavailability Evaluation of Hydroxypyridinonate Actinide Decorporation Agents in Pre-Clinical Pharmacokinetic Studies. *J. Chromatogr. Sep. Tech.* **4,** (2011).
48. Goetz, D. H. *et al*. The neutrophil lipocalin NGAL is a bacteriostatic agent that interferes with siderophore-mediated iron acquisition. *Mol. Cell* **10,** 1033–1043 (2002).
49. Berman, H. M. *et al*. The protein data bank. *Nucleic Acids Res.* **28,** 235–242 (2000).
50. Valiev, M. *et al*. NWChem: a comprehensive and scalable open-source solution for large scale molecular simulations. *Comput. Phys. Commun.* **181,** 1477–1489 (2010).

51. Becke, A. D. Density-functional exchange-energy approximation with correct asymptotic behavior. *Phys. Rev. A* **38,** 3098 (1988).
52. Lee, C., Yang, W. & Parr, R. G. Development of the Colle-Salvetti correlation-energy formula into a functional of the electron density. *Phys. Rev. B* **37,** 785 (1988).
53. Küchle, W., Dolg, M., Stoll, H. & Preuss, H. Energy-adjusted pseudopotentials for the actinides. Parameter sets and test calculations for thorium and thorium monoxide. *J. Chem. Phys.* **100,** 7535–7542 (1994).
54. Godbout, N., Salahub, D. R., Andzelm, J. & Wimmer, E. Optimization of Gaussian-type basis sets for local spin density functional calculations. Part I. Boron through neon, optimization technique and validation. *Can. J. Chem.* **70,** 560–571 (1992).
55. Runge, E. & Gross, E. K. Density-functional theory for time-dependent systems. *Phys. Rev. Lett.* **52,** 997 (1984).
56. Brabec, J. *et al.* Efficient Algorithms for Estimating the Absorption Spectrum within Linear Response TDDFT. *J. Chem. Theory Comput.* **11,** 5197–5208 (2015).
57. Saue, T. *et al.* DIRAC, a relativistic ab initio electronic structure program. *Release DIRAC12* (2012).
58. Dyall, K. G. Relativistic double-zeta, triple-zeta, and quadruple-zeta basis sets for the actinides Ac–Lr. *Theor. Chem. Acc.* **117,** 491–500 (2007).

Acknowledgments

This work was supported by the U.S. Department of Energy, Office of Science Early Career Research Program and Office of Science, Office of Basic Energy Sciences, Chemical Sciences, Geosciences, and Biosciences Division at the Lawrence Berkeley National Laboratory under Contract DE-AC02-05CH11231 (R.J.A.), and by the National Institutes of Health (R01DK073462, R.K.S.). The Radiochemical Engineering and Development Center at Oak Ridge National Laboratory is supported by the U.S. Department of Energy, Isotope Development and Production for Research and Applications Program. The Advanced Light Source (ALS) and Energy Research Scientific Computing Center (NERSC) are supported by the Director, Office of Science, Office of Basic Energy Sciences, of the U.S. Department of Energy under Contract No. DE-AC02-05CH11231. The Innovative and Novel Computational Impact on Theory and Experiment (INCITE) program provided an award of computer time through resources at the Oak Ridge Leadership Computing Facility, a U.S. DOE Office of Science User Facility supported under Contract DE-AC05-00OR22725. We thank M. Allaire, S. Morton, J. Bramble, K. Engle, M. Dupray, and I. Tadesse for assistance in implementing diffraction data collection on radioactive crystals at ALS 5.0.2 beamline.